Proof Delivery Form

Journal and Article number: BOC 428

BC reference: BC2008/0051

Number of colour figures: Nil

Number of pages (not including this page): 12

Biology of the Cell

Please print out your proof, mark any corrections needed, and return it, together with the offprint order form, by FAX to +44 (0)20 7280 4169 as soon as possible (no later than 48 hours after receipt).

- You are responsible for correcting your proofs! Errors not found may appear in the journal.
- The proof is sent to you for correction of typographical errors only, and revision of the substance of the text is not permitted.
- Please answer carefully any queries from the subeditor.
- A new copy of a figure must be provided if correction is required.

Notes:

1. The quality of half-tone and colour figures will be checked by the editorial office.
2. If you have any comments, however minor, on the handling of your paper, please let us know. Please quote the paper's reference number when doing so.
3. If you have any queries, please contact the editorial office by email (editorial@portlandpress.com) or by telephone on 020 7280 4110 (+44 20 7280 4110 from outside the U.K.).

Author queries:

Typesetter queries:

Non-printed material:

Please return this form with your proof

Order for Offprints for *Biology of the Cell*

Article number **BOC**..... No. of pages .....

Reference number **BC200**...../ ..... Title of paper .....

.....

SECTION 1– INFORMATION

Please return this form with your proof to: *Biology of the Cell* Editorial Office, FAX: +44 (0)20 7280 4169
(Portland Press Ltd, Third Floor, Eagle House, 16 Procter Street, London WC1V 6NX, UK).

Offprints must be ordered using this form. If an official order form from your organization is required, it may be sent on later (please quote the article and reference numbers above), but it will be assumed that any such order received is not an additional order. Free offprints are not available and offprints cannot be supplied after publication.

Offprint orders are despatched by surface mail approximately 2 weeks after publication (allow up to 6 months for delivery). If you wish them to be despatched by Airmail please tick the box in section 2 below and add 40% to the indicated price.

If your article contains supplementary online data, please note that any offprints ordered will not include this material.

***Biology of the Cell* 2008 Offprint Order Charges**

Number of pages	Number required [price in Pounds sterling (£)]					
	50	**100**	**200**	**300**	**400**	**500**
1–4	149	194	313	427	531	630
5–8	198	265	427	588	735	884
9–12	258	346	571	805	1012	1218
13–16	322	427	749	1068	1369	1667

Notes

1. For quantities not listed, please ask for a quotation
2. Prices revised October 2007

SECTION 2– ORDER

☐ I do not wish to order offprints of my article

☐ I wish to purchase..... (minimum 50) offprints of my article at a cost of ..... £/$/€

☐ Please send my offprints by Airmail (add 40% to the price indicated) at an additional cost of ..... £/$/€

☐ Bank charges (if applicable, see section 3) ..... £/$/€

Total cost..... £/$/€

Name and address to which offprints should be sent (please enter this information clearly):

.....

.....

.....

.....

.....

SECTION 3– PAYMENT

We accept payment:

- in pound sterling cheques drawn on UK banks
- in US dollar cheques drawn on US banks
- in Euro cheques drawn on any European bank
- by Visa, Mastercard and most major debit cards

Please indicate your preferred payment option:

1 ☐ I enclose a remittance payable to Portland Press Limited

2 ☐ Please send an invoice to the following address (if different from address in section 2)

.....

.....

.....

.....

.....

For payment in $US or Euros, please convert the price shown above at the current rate of exchange and add £15 for bank charges.

3 ☐ I wish to pay by Visa/Mastercard/Visa Delta/Switch/ Maestro (delete as appropriate)

Card number: .....

Name on card: .....

Start date ..... End date .....

Issue no (Switch only): .....

Full address of cardholder:

.....

.....

.....

.....

Cardholder signature ..... Date.....

Biology of the Cell Editorial Office, Portland Press Ltd, Third Floor, Eagle House,16 Procter Street, London WC1V 6NX, UK
Tel: +44 (0)20 7280 4110; fax: +44 (0)20 7280 4169; email: editorial@portlandpress.com; WWW: http://www.portlandpress.com

Biol. Cell (2008) **100**, 00–00 (Printed in Great Britain) doi:10.1042/BC20080051

Research article

Raman microspectrometry sulfur detection and characterization in the marine ectosymbiotic nematode *Eubostrichus dianae* (Desmodoridae, Stilbonematidae)

David Himmel*[1], Leslie Candice Maurin†, Olivier Gros† and Jean-Louis Mansot*

*GTSI - Université des Antilles et de la Guyane, UFR des Sciences Exactes et Naturelles, Département de Physique. B.P. 592. 97159 Pointe-à-Pitre Cedex, Guadeloupe, France, and †UMR-CNRS 7138, Systématique-Adaptation-Evolution, Equipe Symbiose, Université des Antilles et de la Guyane. UFR des Sciences Exactes et Naturelles, Département de Biologie. B.P. 592. 97159 Pointe-à-Pitre Cedex, Guadeloupe, France

Background information. Marine nematodes belonging to the Stilbonematidae (Desmodoridae) family are described as living in obligatory association with sulfur-oxidizing chemoautotrophic ectosymbionts. The symbiotic bacteria carrying out this chemosynthesis should contain elemental sulfur in periplasmic granules as sulfur granules of chemoautotrophic endosymbionts described in various marine invertebrates.

Results. Based on TEM analyses, extracellular bacteria surrounding *Eubostrichus dianae* possess these spherical periplasmic granules. Few investigative techniques can be used to identify elemental sulfur S_8 such as EDXS (energy dispersive X-ray spectroscopy) and EELS (electron energy loss spectroscopy) associated with cryo-fixation of the sample to avoid sulfur loss. These techniques are time consuming, expensive and require technical skills. Raman microspectrometry applied to the analysis of *E. dianae* allowed us to detect elemental sulfur S_8 and confirmed the location of these sulfur clusters in the bacterial coat. In the same way, Raman spectrometry was positively applied to the endosymbiotic bivalve *Codakia orbicularis,* suggesting that this technique can be used to characterize sulfur in ecto- as well as in endo-symbiotic sulfur-oxidizing bacteria.

Conclusions. As Raman spectrometry can be used on living organisms (without preliminary fixation) without sample damage and preserving the molecular structure of the sulfur (denatured during chemical fixation) it represents a very well-adapted investigative tool for biologists. This technique therefore permits us to detect quickly and easily (in a few seconds and on entire living animals) the presence of sulfur compounds in the symbiotic nematode.

Introduction

Several marine organisms living in sulfidic environments are associated with symbiotic bacteria. In the benthic deep-sea environment as hydrothermal vents, cold seeps and whale bones, many associations between marine invertebrates and proteobacteria have been described such as in arthropods (Bresiliidae) (Polz and Cavanaugh, 1995; Zbinden et al., 2004), polychaetous annelids (Alvinellidae) (Desbruyères et al., 1983; Cary and Stein, 1998) or in bivalve molluscs (Mytilidae, Vesicomyidae) (Felbeck et al., 1981; Cavanaugh, 1983; Deming et al., 1997) etc. Similar relationships have also been described in tropical coastal environments in bivalvia (Lucinidae) (Berg and Alatalo, 1984; Reid, 1990) and in

[1]To whom correspondence should be addressed (email dhimmel@univ-ag.fr).
Key words: bacterium, elemental sulfur detection, marine invertebrate, Raman microspectrometry, symbiosis.
Abbreviations used: ATEM, analytical transmission electron microscopy; cTEM, conventional transmission electron microscopy; EELS, electron energy loss spectroscopy; EFTEM, energy-filtered transmission electron microscopy; SEM, scanning electron microscopy; TEM, transmission electron microscopy.

nematoda (Stilbonematidae) (Ott and Novak, 1989; Ott et al., 1991). These thiotrophic organisms depend on the chemoautotrophic metabolism of reduced sulfur compounds and form symbiotic relationships with sulfur-oxidizing bacteria (Vetter, 1991).

The nature of invertebrate bacterial symbionts living in a low-sulfidic environment is classically determined using analytical electron microscopy [SEM (scanning electron microscopy), TEM (transmission electron microscopy) and EDXS (energy dispersive X-ray spectroscopy)], biochemical analyses, enzymatic studies and phylogeny (Cavanaugh, 1985; Polz et al., 1992; Bauer-Nebelsick et al., 1996a, 1996b; Rinke et al., 2006). The studies carried out on stilbonematids supposed that bacterial symbionts are thio-autotrophic γ-proteobacteria (Ott et al., 1991; Polz et al., 1992; Ott et al., 2004); however, only two studies were reported using 16S rDNA (ribosomal DNA) sequence analysis. The first results obtained on the nematode *Laxus sp*. permit design of a specific probe from a single bacterial sequence (Polz et al., 1994). The second phylogenetic analyses on the nematode *Eubostrichus dianae* have not really been conclusive (Polz et al., 1999). Owing to the microscopic size of nematodes, all techniques used for the DNA extraction of the symbionts require a large quantity of worms (100–200 individuals per assay). Moreover, filamentous bacteria that densely covered the entire surfaces of the nematodes were not detected by PCR-based analysis. So, specific probes and/or primers of these ectosymbiotic bacteria cannot be designed. Nevertheless, ultrastructural studies (TEM) of these nematodes indicate that such ectosymbiotic bacteria contain spherical cytoplasmic inclusions (Polz et al., 1992). These electron-lucent inclusions resemble sulfur globules found in the chemoautotrophic symbionts described in some bivalves (Vetter, 1985) and oligochaetes (Giere et al., 1988), as well as free-living sulfur-bacteria such as *Beggiatoa* (Lawry et al., 1981). These data suggest that such bacteria belong to the sulfur-oxidizing group.

Additional techniques focusing on the functional genes [APS (5′ adenylylsulfate) reductase] and the detection of elemental sulfur by high-pressure freezing of organisms, followed by a freeze-substitution and cryo-embedding before a cryo-EFTEM (energy-filterered TEM) microanalysis have recently been published (Lechaire et al., 2006, 2008). The main problem for the detection of sulfur is that the solvents, such as ethanol, used during dehydration of samples before epoxy-resin embedding dissolve sulfur compounds (Truchet et al., 1998; Pasteris et al., 2001). Moreover, the techniques used for this detection require a high technical skill, heavy sample preparation, and are consequently time consuming and expensive.

White et al. (2006) have shown the capabilities of Raman spectrometry to investigate sulfur S_8 in biological materials by *in situ* analysis in deep ocean. The present study is concerned with the detection, identification and location of elemental sulfur in freshly collected biological samples by means of Raman microspectrometry. The main advantages of this visible light spectrometry are that it can be quickly applied to biological samples in their original environment (i.e. in seawater) without any specific preparation. The spectra can be acquired in a short time (few seconds) on small areas without sample damage.

The technique is applied to the ectosymbiotic nematode *E. dianae* (Hopper and Cefalu, 1973) for which no data are available concerning sulfur contents and to the endosymbiotic bivalve *Codakia orbicularis* (Linné, 1758) known to harbour sulfur-oxidizing gill-endosymbionts (Berg and Alatalo, 1984; Frenkiel and Mouëza, 1995), containing elemental sulfur granules as recently determined by EELS (electron energy loss spectroscopy) (Lechaire et al., 2008). Contrary to the study of Pasteris et al. (2001) our present study focuses directly on entire organs or small individuals (meiofauna).

Results and Discussion

Characteristics of the nematode

The nematode *E. dianae* presents extremely long filaments which form a coat around the body of the worm (Figures 1a and 1b). The ectosymbiotic bacteria comprising this coat have a length of 80–100 μm and a diameter of 0.5–1 μm. We can observe on Figure 1(a) the white appearance of the bacterial coat in optical microscopy and in Figure 1(b) the uniform shape of bacteria arranged regularly on the cuticle of the nematode.

Raman analysis applied to living nematode

In order to detect and localize sulfur on this ectosymbiotic nematode 30 Raman spectra were recorded across the living nematode. The laser probe diameter was 10 μm and the distance between two successive

Figure 1 | Raman characterization and location of sulfur in living ectosymbiotic *Eubostrichus dianae*

(**a**) Light microscopy view of an entire nematode *E. dianae*. The bacterial coat appears white whereas the body of the nematode (indicated with*) is dark grey. Owing to the use of a cover glass for the observation, the bacterial coat is flattened and it appears thicker (approx. 100 μm compared with 30 μm normally). (**b**) SEM micrograph of the midbody region of *E. dianae* showing the long filament cells forming the bacterial coat surrounding the entire body of the nematode. The superimposed white circles indicate the size and position of the Raman probe used for the profile acquisition. (**c**) Three rough spectra extracted from the Raman profile data pointing out the presence of sulfur in the nematode, whereas no sulfur is detected in the surrounding water. The pure sulfur (S_8) spectrum presenting three intense Raman characteristic bands (arrows) is shown as a reference as dotted lines. (**d**) The intensity of the sulfur 480 cm^{-1} Raman line as a function of the probe position. The curve, representative of the sulfur content in the probed volume, demonstrates the presence of sulfur in the bacterial-bearing nematode. It presents two

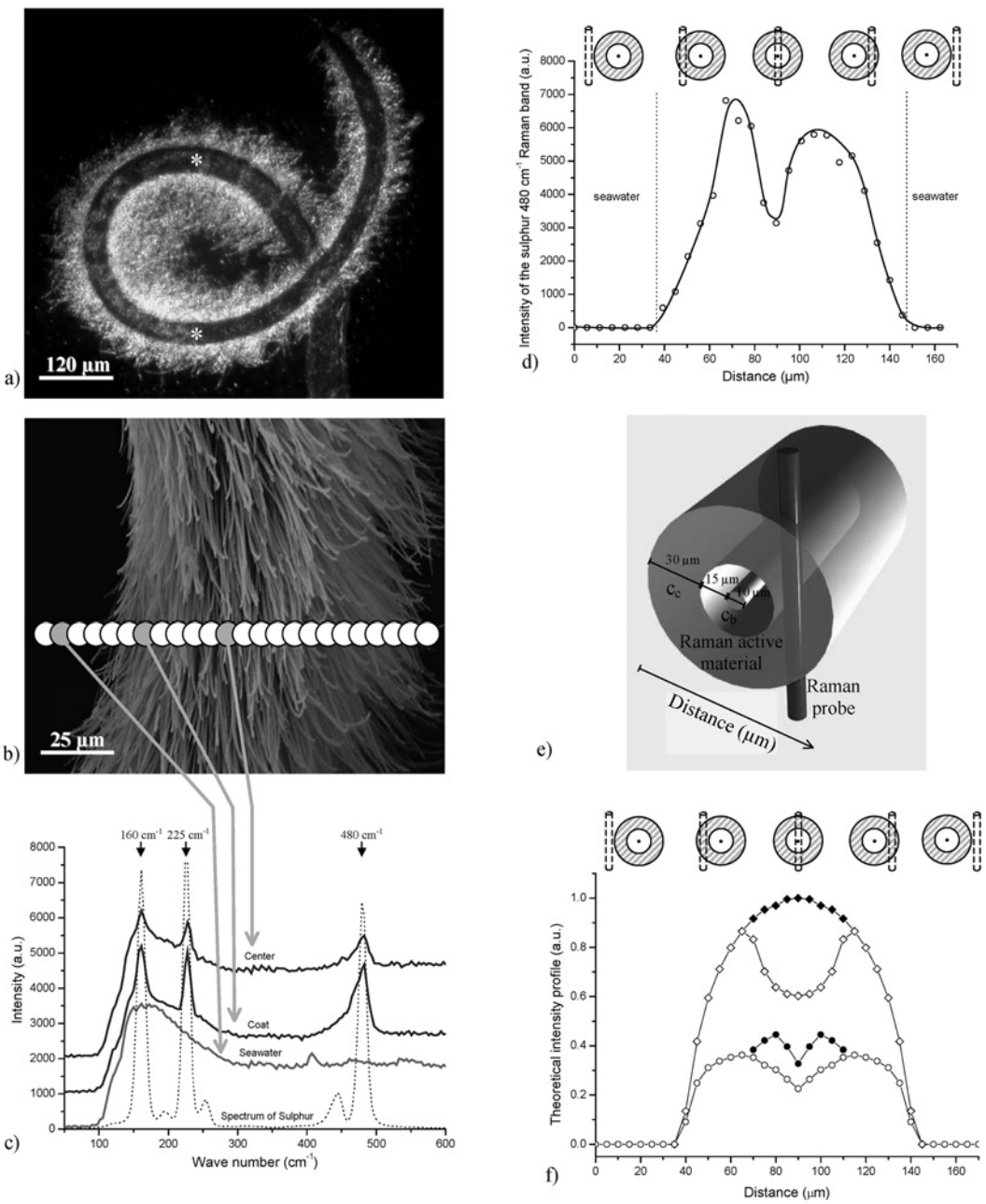

maxima separated by a valley corresponding approximately to the center of the nematode. (**e**) Schematic representation of the body of the nematode surrounded by its bacterial coat. (**f**) Theoretical intensity profile of the sulfur characteristic band deduced from the model (**e**) assuming the linear relationship between intensity and sulfur amount and homogenous sulfur distribution in the analysed volumes (sulfur concentrations c_c in the body of the nematode and c_b in the bacterial coat). The theoretical profiles presented correspond to: (●, ◆), $c_b = c_c = 1$ (a.u.); and (○, ◇), $c_b = 0 \& c_c = 1$ (a.u.), for a perfectly transparent (◆, ◇) and absorbing sample (●, ○). a.u. arbitrary unit.

analyses was 5.6 μm. The white circles drawn on the SEM micrograph (Figure 1b) illustrate the size and location of the probe used to acquire the Raman profiles on the living animal.

Figure 1(c) shows a selection of three representative Raman spectra recorded in seawater (near the nematode), on the bacterial coat and in the middle part of the nematode (including the probed volume of the nematode body and twice the bacterial coat) respectively. The Raman spectra obtained on the bacterial coat and the midbody of the nematode present three Raman bands (at 160 cm^{-1}, 225 cm^{-1} and 480 cm^{-1}) characteristic of the presence of sulfur S_8 (Poborchii, 1996). These bands are not present in the spectra of seawater (Figure 1c).

As already mentioned in previous work (Long, 1977), the intensity of a Raman scattering band characteristic of a compound is linearly related to its amount contained in the analysed volume. This fact is used to locate S_8 in *E. dianae*. The diagram shown in Figure 1(d) represents the variation of the intensity of the S_8 480 cm^{-1} Raman band as a function of the position of the laser probe on the sample (equivalent diagrams are obtained using the intensity of the two other peaks at 160 cm^{-1} and 225 cm^{-1}).

The zero intensity points on this diagram (no sulfur) correspond to the analyses outside of the sample. Sulfur is detected over a distance of 100 μm corresponding to the diameter of the body of the nematode (40 μm) surrounded by its bacterial coat (thickness 30 μm). The intensity profile across the sample reveals two maxima separated by a valley corresponding to the centre of the nematode.

Spatial interpretation of the Raman results

In order to interpret this diagram, the nematode and its bacterial coat are schematically drawn in Figure 1(e). The body of the nematode is represented by a 40 μm diameter cylinder surrounded by the bacterial coat of 30 μm thickness. The laser probe is represented by a vertical cylinder crossing the sample. For simplification sulfur is considered to be homogeneously dispersed at the probe scale level, at a concentration c_b in the nematode body and c_c in the bacterial coat.

The Raman scattered intensity is proportional to the exciting line intensity and to the amount of sulfur contained in the probed volume, i.e. the intersection volume between the cylinder representing the probe and the schematized sample multiplied by the local sulfur concentration (see the section 'Quantitative interpretation of the spectra' below). In the case of a perfectly transparent sample, the intensity of the incident exciting line is considered constant across the sample and the Raman scattering intensity is just proportional to the probed volume multiplied by the local concentration. In the case of an absorbing sample the results must be corrected from absorption phenomena. The local exciting line intensity and Raman scattering damping must be calculated taking into account the absorbing properties of the medium. The experimental and mathematical developments for this purpose are reported below in the section 'Influence of the light absorption by the various parts of the sample on the Raman scattering intensity'.

Figure 1(f) presents theoretical Raman intensity profiles for the two following cases: $c_b = c_c = 1$ [a.u. (arbitrary unit)] and $c_b = 0$ & $c_c = 1$ (a.u.). The theoretical profiles are calculated assuming a perfectly transparent sample and considering an absorbing sample using the mathematical expression and experimental absorption coefficients presented in the paragraph 'Mathematical expression of the Raman scattered light intensity for an idealized ectosymbiotic nematode'.

The main effects of the absorption properties of the various parts of the sample (bacterial coat, nematode body and digestive tube) is the important reduction (~50 %) of the Raman scattered intensity. The difference between the two theoretical corrected profiles

[$c_b = c_c = 1$ (a.u.) and $c_b = 0$ & $c_c = 1$ (a.u.)] is the relative intensity changes (Δ) between Raman intensity maxima I_M and minima I_m:

$$\Delta = \frac{I_M - I_m}{I_M}$$

For $c_b = c_c = 1$ (a.u.), $\Delta = 0.27$, and for $c_b = 0$ & $c_c = 1$ (a.u.), $\Delta = 0.38$.

This last value agrees well with the experimental variation recorded on the sample (Δ=0.41) and strongly supports the absence of sulfur in the body of the nematode and its digestive tube.

This conclusion is confirmed by the Raman spectra recorded on to a nematode where the bacterial coat was accidentally eliminated during sample manipulation. In that case, the spectra do not exhibit any characteristic line of sulfur demonstrating that the body of the nematode is effectively sulfur free (results not shown).

The non-symmetrical shape of the experimental intensity profile can be attributed to the irregular distribution of the bacteria around the body of the nematode as pointed out on the SEM micrograph (Figure 1b).

Raman and EELS investigations on embedded nematode

Thus Raman microspectrometry analyses carried out on the nematode *E. dianae* allowed us to detect the elemental sulfur S_8 in living samples and to localize this compound in the bacterial coat. Owing to the size of the probe compared with the size of the bacteria, it was not possible to show whether this elemental sulfur was located inside (i.e. in the cytoplasm or within granules inside the periplasmic space) or outside the bacteria as previously described in symbiotic bivalves with cryo-EFTEM microanalysis + EELS (Lechaire et al., 2006, 2008).

In order to emphasize the advantages of Raman microspectrometry applied to living nematode, compared with classical ATEM (analytical TEM), Raman microspectrometry is applied to a semi-thin section of classically prepared samples in order to demonstrate the loss of sulfur induced by the sample preparation process.

The light and transmission electron micrographs presented in Figures 2(a) and 2(b) were obtained on cross-sections of nematodes embedded in LR White resin. Semi-thin and thin sections for Raman and ATEM investigations were both obtained from the same block.

A Raman scan analysis was performed on the semi-thin section of *E. dianae*. Twenty spectra were recorded across the LR White resin, the bacterial coat and the body of the nematode (Figure 2a). The study of the twenty spectra obtained during the scan demonstrated the lack of the three characteristic peaks of sulfur (Figure 2d), pointing out the absence of sulfur S_8 in the sample.

The same result was observed on samples analysed by EELS. On the ultra-thin section, no sulfur was detected in the body of the nematode, in the bacterial coat or in the granules included in each bacterial symbiont.

As expected, neither EELS (Figure 2c) nor Raman spectroscopy (Figure 2d) analyses carried out on various parts of the sample allowed us to detect sulfur. This clearly confirms that sample preparation for ATEM investigation is responsible for the loss of sulfur. Sulfur S_8 is known to be soluble in ethanol, a solvent commonly used in cTEM (conventional TEM) after chemical fixation, during ethanol dehydration and epoxy-resin embedding of biological samples (Vetter, 1985; Truchet et al., 1998; Pasteris et al., 2001). Consequently, the small electron-lucent granules within the bacterial symbiont usually appear empty in ultra-thin sections.

The observations show that these techniques are inefficient on embedded organisms after chemical fixation; however, EELS on cryo-fixed samples allows precise location of compounds (Lechaire et al., 2006; 2008). Nevertheless, Raman microspectrometry is the easiest technique which provides a positive result in a few seconds from an entire animal and without heavy sample preparation, permitting an easy and fast screening of sulfur in biological samples.

Raman analysis on endosymbiotic bivalve

In order to confirm the efficiency of Raman microspectrometry for detection of elemental sulfur in any kind of sulfur-oxidizing symbiotic organisms, we applied this technique to an endosymbiotic model. We used the tropical bivalve *C. orbicularis*, which lives in the same low sulfidic environment as *E. dianae* but harbour intracellular thiotrophic bacteria inside specific cells of the gill tissue (Frenkiel and Mouëza,

Figure 2 | Raman and EELS sulfur investigation on embedded ectosymbiotic *Eubostrichus dianae*

(**a**) Light microscopy of a longitudinal semi-thin section (0.5 μm thickness) of *E. dianae* embedded in LR White resin. The filamentous bacterial coat is situated on the cuticle (cu) of the nematode which presents various organs inside its body. The Raman scan consisting of 20 spectra over a total distance of 158 μm is illustrated by white circles. (**b**) TEM of a transversal 60 nm section of *E. dianae* embedded in LR White resin. View of the empty digestive track (DT), and various organs free of bacteria inside the body of the nematode. The extracellular bacterial coat surrounding the cuticle (cu) of the nematode is composed of transverse (black arrow) and longitudinal (white arrow) sections of the same species. Insert: high magnification of transverse sections of a few bacteria with periplasmic electron-lucent granules (*) that normally contain the elemental sulfur (detected by Raman microspectrometry in living individuals). (**c**) EELS collected on the same thin section presented in (**b**). No sulfur is detected in the body of the nematode, the bacterial coat and on a periplasmic electron-lucent granule (Ahn and Krivanek, 1983). (**d**) Series of Raman spectra collected across the embedded sample. The dotted line indicates the reference sulfur (S_8) spectrum. As in the EELS investigation, no sulfur is revealed in the sample.

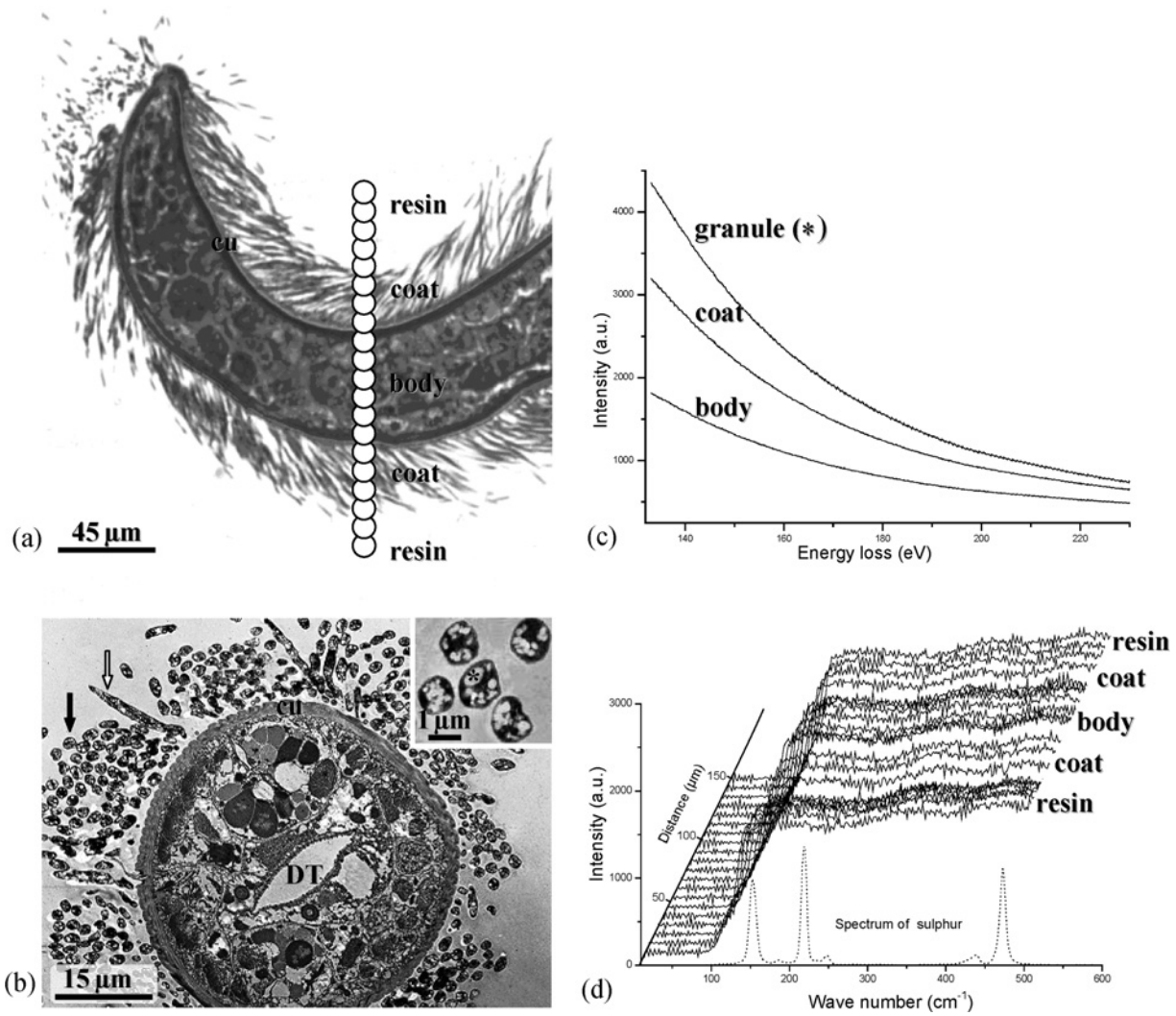

1995). In the eulamellibranch bivalve *C. orbicularis*, the gills are thick and cover almost completely the visceral mass (Reid, 1990). As previously described by Frenkiel and Mouëza (1995), bacteriocytes represent one of the major cell types of the gill filament (Figure 3b) of *C. orbicularis*. The bacteriocytes, mostly located in the one-third of the lateral zone, possess a cytoplasm filled with intracellular bacteria

Figure 3 | Sulfur detection by Raman microspectrometry on the gill-endosymbiotic bivalve *Codakia orbicularis*
(**a**) Overview of a freshly collected adult individual of *C. orbicularis* in which one valve was removed. The large and thick creamy gill (G) characteristic of lucinid bivalves occupies the main volume of the palleal cavity. F, foot; M, adductor muscles; Ma, mantle; sw, seawater. (**b**) Light micrograph of gill filaments from a freshly collected *C. orbicularis* after Goldner staining. The ciliated zone (CZ) characterized by numerous cilia is devoided of bacteria. The first one-third of the lateral zone (LZ) contains mostly bacteriocytes (BC) harbouring bacterial symbionts, whereas the two other thirds contain mucocytes in blue (*) and granule cells (GC). (**c**) cTEM view of two bacteriocytes (BC) of the lateral zone of a gill filament from a freshly collected *C. orbicularis*. Bacteriocytes (BC) have an apical pole with short microvilli (mv) developing a broad contact with pallial sea-water (sw). The cytoplasm is crowded by thioautotrophic bacteria (b) that are usually individually enclosed inside bacteriocyte vacuoles. Intercalary cells (IC) that are regularly interspersed between bacteriocytes are devoid of bacterial symbionts. (**d**) Raman spectra collected in gill and the surrounding water showing the presence of the S_8 characteristic lines only in the gill. a.u. arbitrary unit. (**e**) Intensity profile of the 225 cm^{-1} sulfur Raman line as a function of the probe position. It clearly demonstrates the presence of sulfur in the gill, whereas no sulfur is detected outside.

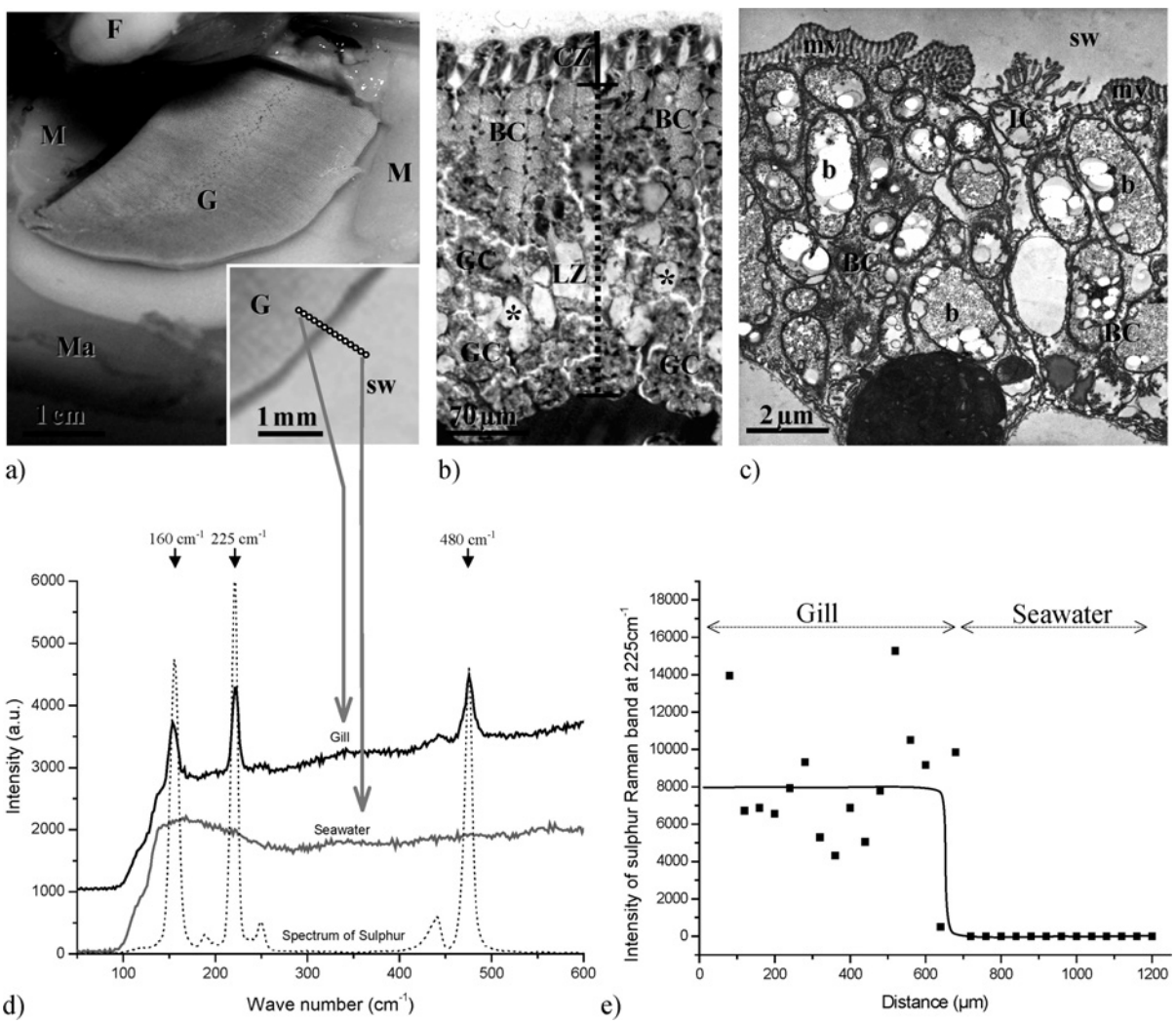

characterized by numerous periplasmic empty vesicles (Figure 3c). This host cell is characterized by an apical pole bearing short microvilli in contact with the circulating seawater and few mitochondria as host organelles. Bacteria are usually individually enclosed and present the double membrane typical

for Gram-negative bacteria (Figure 3c). The bacterial cytoplasm usually contains essentially DNA, ribosomes and empty clear granules located in the periplasmic space (Figure 3c) which are considered as sulfur granules according to their appearance with cTEM.

The insert of Figure 3(a) shows the location of the probe used to acquire the sulfur concentration profile. The two spectra in Figure 3(d) correspond to analyses in water and in the gill of *C. orbicularis*. Sulfur is clearly detected in this tissue, whereas no sulfur is detected in the surrounding water. The full intensity profile of the sulfur 225 cm^{-1} characteristic Raman line as a function of the probe location is presented in Figure 3(e). This obviously demonstrates the presence of sulfur in the gills of *C. orbicularis* which was previously located in the periplasm of the sulfur-oxidizing bacterial endosymbionts by Lechaire et al. (2008).

Conclusions

Detection and characterization of sulfur in thioautotrophic bacteria is of interest in the understanding of symbiotic relationships in marine invertebrates colonizing sulfidic environments.

Further investigations will focus on the use of such techniques to assume potential sulfur-oxidizing bacterial symbiotic interactions in organisms belonging to the meiofauna not yet described as symbiotic.

In the present study we demonstrated that Raman microspectrometry is a powerful tool for such a purpose. It allowed us to point out the presence of elemental sulfur in the biological samples, to identify its structure as the S_8 species and to locate it in the samples with an actual spatial resolution of 10 μm.

This resolution will be improved down to 2 μm in the next few months. This ultimate spatial resolution will not allow us a precise location of sulfur at the ultrastructural level as it can be done by means of cryo-EFTEM microanalysis. Nevertheless even with a 10 μm resolution it permits detection and characterization of the speciation of sulfur and locates it at mesoscale within a very short time.

The main advantages of this technique are: (i) its possible application on living samples in their natural environment (in the present study seawater); (ii) its non-destructive nature (interaction of visible light with sample); (iii) its short acquisition time (a few seconds to a few minutes depending on the exciting line power and sulfur concentration); and (iv) its capability to extract chemical species maps or profiles with spatial resolution in the micrometre range.

Materials and Methods

Collection of material

E. dianae (Hopper and Cefalu, 1973) and *C. orbicularis* (Linné, 1758) were both collected from the tropical seagrass bed of *Thalassia testudinum*. The tropical site is the 'îlet cochon' located in the 'petit cul de sac marin' in Guadeloupe (French West Indies, Caribbean).

Bivalves were manually collected, whereas nematodes were extracted by sieving on a 2 mm mesh from a 145 mm diameter core of sediment. The nematode *E. dianae* were extracted using a binocular microscope and were re-suspended in filtered seawater (0.22 μm) before analysis.

Electron microscopy (SEM, TEM) techniques

Sample preparation methods

For TEM, individuals were fixed for 3 h at 4°C in 4% (w/v) paraformaldehyde in 0.22 μm filtered seawater. After two washes in sterile seawater at room temperature (24°C) and dehydration through an ascending ethanol series, they were embedded in hydrophilic LR White resin (Biovalley) as previously described (Gros and Maurin, 2008). Sections (60 nm) were stained for 30 min in 2% aqueous uranyl acetate and 10 min in 0.1% lead citrate before examination in a Philips 201 microscope running at 75 kV. Semi-thin sections were stained with Toluidine Blue in 1% borax buffer and observed on a Nikon epi80i light microscope.

For SEM, animals were fixed as described above before dehydration in an acetone series and critical-point drying. Samples were then gold coated (sputtering) before observation with a SEM S2500 Hitachi running at 20 kV.

An overall view and histological information was obtained from 7 μm paraffin sections. A gill dissected from one individual, was fixed in Bouin's fluid (Gabe, 1968) for 24 h at room temperature, and was then embedded in paraplast before histological staining according to Frenkiel and Mouëza (1995).

EFTEM

Thin sections from a LR white resin block were investigated with a LEO 912 TEM microscope. An Omega transmission electron microscope (LEO Electron Optics GmbH, Oberkochen, Germany) equipped with a LaB_6 source, and operated at 120 kV was used. The LEO 912 features an in-column spectrometer [magnetic omega-type electron energy-loss filter (Egerton, 1986; Crozier, 1995)]. PEELS (parallel electron energy loss spectra) were recorded with a cooled slow-scan CCD (charged-coupled device) camera operating in 14-bit mode. The Omega filter was adjusted to obtain an energy resolution of 1.5 eV.

Raman microspectrometry

Outline of the technique

Raman spectrometry is based on an inelastic light/matter interaction (Figure 4). It allows us to probe the vibrational

Figure 4 | Schematic diagram of the principle of a Raman experiment

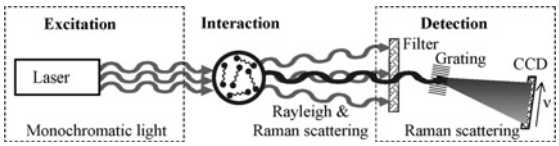

energy levels of materials, i.e. molecular or crystalline bonding. The probed material can either be in the gaseous, liquid or solid state. This spectrometry cannot be applied to metallic compounds.

Figure 5 shows the quantum mechanics representation of the main interaction processes of light with a molecule.

Spectrometry sensitivity

The sensitivity of Raman spectrometry is highly dependent on the probed compound and especially on the energy difference ΔE between ground and excited electronic levels. When the energy of the exciting photons is far from ΔE, 'normal' Raman scattering occurs, intensity represents about 10^{-6} of the intensity of the incident light leading to a relatively low sensitivity (Figure 5).

When the energy of the incident photon is close to ΔE, pre-resonance or resonance Raman scattering occurs and the Raman scattering intensity can be enhanced by a factor of 10^2–10^3, increasing by the way the sensitivity of the method (Long, 1977).

The choice of Raman as the analytical technique used to identify and locate sulfur in low concentrations in biological samples has been induced by the fact that sulfur in the S_8 structure presents pre-resonance Raman scattering (Herzberg, 1945).

Raman scans

Computer-controlled acquisition and data analysis treatment were developed at GTSI in order to acquire Raman profiles and maps. For this purpose Raman point spectra are acquired along lines in the case of profiles and along several lines covering a whole rectangular area in the case of a mapping (Himmel, 2005).

Quantitative interpretation of the spectra

It has been demonstrated previously (Himmel, 2005) that the probe geometry in the experimental conditions of this work can be represented by a cylinder of 120 μm length by 10 μm diameter. In the case of an homogeneous and transparent sample, the intensity of a characteristic Raman line is linearly related to the analysed volume. In the case of an absorbing sample the intensity of the Raman lines must be corrected by the local attenuation of the exciting line and Raman scattered light. Taking into account the diameter of the nematode, the thickness of its bacterial coat and the exciting line attenuation profile in the sample Raman spectra treatment will allow us to determine the location of sulfur.

Figure 5 | Simplified energy bands diagram for a diatomic molecule and schematic representation of the main processes of photon/matter interactions

Absorption/fluorescence phenomena (I): the incident photon has an energy $h\nu_i$ sufficient to initiate a dipolar transition from an electronic ground state to excited state. The return of the molecule to its ground state results in the emission of a fluorescence photon with an energy lower than the incident one (fluorescence emission). Scattering phenomena (II and III): the energy $h\nu_0$ of the incident photon is not sufficient to initiate the transition between the electronic ground state and the excited state. Rayleigh scattering process (II): the transition from an initial vibrational state to the same final one via a virtual excited state results in the scattering of the photon at the same energy $h\nu_0$. Raman scattering: (III-1, III-2): the transition from an initial state to a different final one always via virtual excited level results in the scattering of a photon with an energy lower (Stokes II-2) or upper (anti-Stokes II-3) than the incident one. The loss or gain in energy undergone by the photon during the scattering process is equal to the energy difference between the initial and the final vibrational levels and then characteristic of the bonded species and type of bonding. These energy quanta can be theoretically calculated taking into account the atomic mass and bonds strength.

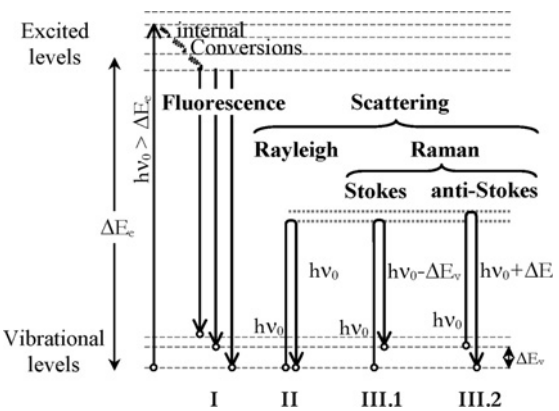

Influence of the light absorption by the various parts of the sample on the Raman scattering intensity

In order to evaluate the absorption of incident laser light as well as the Raman scattered one, we first recorded an optical micrograph of the ectosymbiotic nematode in transmission mode. White light for illumination and a green pass band filter was used ($514\ \text{nm} < \lambda < 556\ \text{nm}$) to analyse the transmitted light (Figure 6a).

The intensity of the transmitted light through the bacterial coat, the nematode body (close to the digestive tube) and the body, including the digestive tube, are measured using free Gwyddion software.

Figure 6 | Light-transmission analysis

The optical micrograph of an ectosymbiotic nematode obtained in transmission using a green light filter is given in (**a**). For light-transmission analysis two light intensity profiles are extracted (**b**) by means of Gwyddion software. The first profile crosses the body completely covered by bacteria, the second one crosses the sample on a part where the bacterial coat was removed. These analyses allow us to experimentally measure the absorption coefficients μ of the different parts of the sample reported in (**c**) and expressed in intensity light unity (ilu).

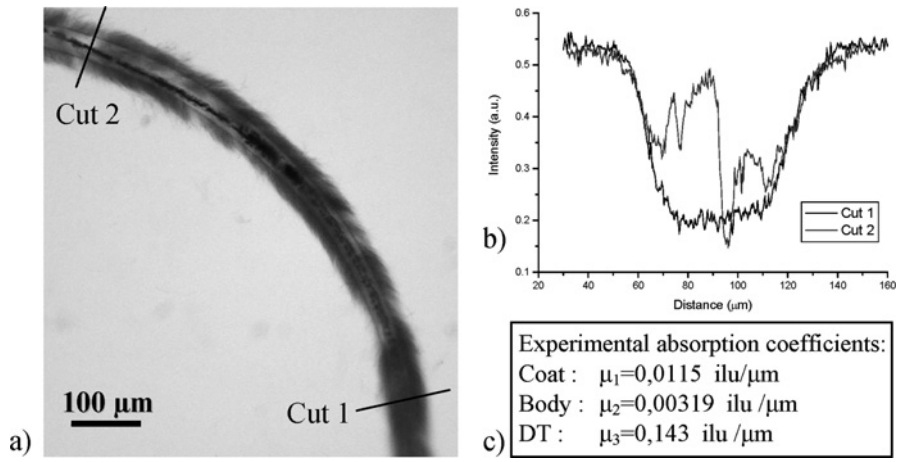

Figure 6(b) shows two transmitted light intensity profiles corresponding to lines crossing the nematode surrounded by its bacterial coat and a part of the nematode where the bacterial coat has been removed.

Assuming that the transmitted light intensity is controlled by the Lambert Beer law:

$$I = I_0 e^{-\mu x}$$

I_0 being the incident light intensity, μ the absorption coefficient, x the thickness of matter crossed by the light and I being the intensity of the transmitted light through the thickness x. We can deduce from the 'green light' optical micrograph the absorption coefficient μ corresponding to each part of the sample. The obtained data are summarized in Figure 6(c). Using these coefficients and applying the Lambert Beer formula for all contributions of the samples' parts (bacterial coat, nematode body, digestive tube) the exciting line intensity can be calculated point by point.

The frequency of the Raman scattered light of interest ($536 < \text{lambda} < 546$ nm) lying in the frequency range of the pass band filter used for the recording of the nematode micrograph, the Lambert Beer equation is also applied to the damping of the Raman scattered light using the absorption coefficients deduced previously (Figure 6C). The full equations are given in the following section.

Figure 7 | Schematic cross-section of the idealized ectosymbiotic nematode

μ_1, μ_2 and μ_3 are the extinction coefficients corresponding to the bacterial coat, the nematode body and the intestine. The x co-ordinates allow us to express the optical pathways of light in the sample.

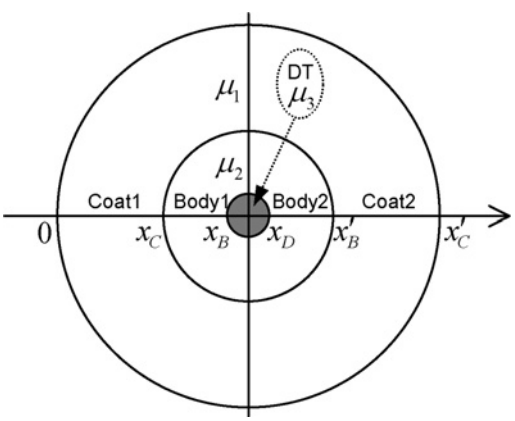

Mathematical expression of the Raman scattered light intensity for an idealized ectosymbiotic nematode

In order to express the Raman scattered light intensity which takes into account the light absorption by the sample, the Lambert Beer law equation is applied to an idealized composite sample where the various parts (bacterial coat, nematode body, digestive tube) are considered homogeneous. Figure 7 presents the cross-section of the idealized nematode and the parameters used in the equations.

As previously mentioned the intensity of light crossing a thickness x of absorbing medium with an absorption coefficient μ is given by the Lambert Beer law (see above).

Applied to the different parts of the nematode for the incident exciting line and Raman scattered light we can calculate the Raman intensity scattered by the various parts of the sample. The corresponding equations are given below, where: I_R is the Raman intensity outgoing from the illuminated sample, σ is the Raman cross-section of the studied species (in the present study this is S_8), and c is the concentration of S_8 in the various parts of the sample.

The thickness crossed by light in the various parts of the sample (Figure 7) are noted: x_C (coat1), $x_B - x_C$ (body1), $x_D - x_B$ (DT, digestive tube), $x'_B - x_D$ (body2) and $x'_C - x'_B$ (coat2):

$$I_{R\ Coat1} = \sigma\,[c]\,I_0 \int_0^{x_C} e^{-2\mu_1 x}\,dx = \sigma_c \frac{I_0}{2\mu_1}(1 - e^{-2\mu_1 x_C})$$

$$I_{R\ Body1} = \sigma_c\, I_0 e^{-\mu_1 x_C} \int_{x_C}^{x_B} e^{-2\mu_2 (x - x_C)}$$

$$dx = \frac{\sigma_c\, I_0 e^{-\mu_1 x_C}}{2\mu_2}\left(1 - e^{-2\mu_2 (x_B - x_C)}\right)$$

$$I_{R\ DT} = \frac{\sigma_c\, I_0 e^{-\mu_1 x_C} e^{-\mu_2 (x_B - x_C)}}{2\mu_3} \int_{x_B}^{x_D} e^{-2\mu_3 (x - x_B)}$$

$$dx = \frac{\sigma_c\, I_0 e^{-\mu_1 x_C} e^{-\mu_2 (x_B - x_C)}}{2\mu_3}\left(1 - e^{-2\mu_3 (x_D - x_B)}\right)$$

and analogue:

$$I_{R\ body2} = \frac{\sigma_c\, I_0 \left(e^{-2\mu_1 x_C} e^{-2\mu_2 (x_B - x_C)} e^{-2\mu_3 (x_D - x_B)}\right)}{2\mu_3} \times \left(1 - e^{-2\mu_2 (x'_B - x_D)}\right)$$

$$I_{R\ coat2} = \frac{\sigma_c\, I_0 \left(e^{-2\mu_1 x_C} e^{-2\mu_2 (x_B - x_C)} e^{-2\mu_3 (x_D - x_B)} e^{-2\mu_2 (x'_B - x_D)}\right)}{2\mu_3} \times \left(1 - e^{-2\mu_1 (x'_C - x'_B)}\right)$$

The total Raman intensity detected after a pathway constituted by the succession coat1, body1, digestive tube, body2, coat2 is expressed by the following sum:

$$I_{R\ total} = I_{R\ coat1} + I_{R\ body1} + I_{R\ DT} + I_{R\ body2} + I_{R\ coat2}$$

The results are shown in Figure 1(f).

Experimental procedure

For the present study, a Raman microspectrometry is used (HR800 HORIBA Jobin Yvon Microspectrometer) allowing us to obtain high spatial resolution analyses (probe diameter 10 µm). The exciting monochromatic light is the 532 nm wavelength radiation emitted by a 5 W NdYag laser (Spectra-Physics Millennia Pro 5 sJS). The laser power on the sample was limited to 40 mW to avoid sample damage. A 600 lines per ml grating was used, allowing recording of a one shot spectrum over an energy range of 0 cm^{-1} to 1720 cm^{-1}, the spectrometer entry slit width was 500 µm leading to a resolution of 1.5 cm^{-1}. The confocal hole diameter used was 500 µm leading to a probe length of 400 µm, well adapted to the diameter of the studied samples. The acquisition time was 7 s, to obtain a good signal-to-noise ratio. To prevent damage induced by overheating, samples were maintained in seawater, which constitutes a good cooling isotonic medium for marine invertebrates. The spectra of the seawater are recorded separately and then can be removed from the spectra acquired on the sample in seawater.

Other potential Raman microspectrometry applications in biology

Raman spectrometry permits molecular and structural analysis and can be adapted to function in different atmospheres. In biology this technique can be applied to the identification of mineral phases such as the constituent of mollusc shells or the mineral content of the digestive tube.

At the level of identification of biological molecules and their distribution, Raman spectrometry can mainly be used in the case of molecules presenting high-intensity Raman spectra, i.e. coloured molecules such as metalloproteins or metal chelates.

Acknowledgements

We would like to thank Y. Bercion and K. Delbé for their technical support.

Funding

This work was supported by the Region Guadeloupe the European Social Fund [grant number CAB/AA/JL/N°02-9]; and the European Regional Development Fund [grant number A-31-44 présage 6257].

References

Ahn, C.C. and Krivanek, O.L. (1983) EELS Atlas, a Reference Guide of Electron Energy Loss Spectra Covering All Stable Elements. Gatan Inc., Warrendale, U.S.A.

Bauer-Nebelsick, M., Bardele, C.F. and Ott, J.A. (1996a) Redescription of *Zoothamnium niveum* (Hemprich & Ehrenberg, 1831) Ehrenberg, 1838 (Oligohymenophora, Peritrichida), a ciliate with ectosymbiotic, chemoautotrophic bacteria. Eur. J. Protistol. **32**, 18–30

Bauer-Nebelsick, M., Bardele, C.F. and Ott, J.A. (1996b) Electron microscopic studies on *Zoothamnium niveum* (Hemprich & Ehrenberg, 1831) Ehrenberg, 1838 (Oligohymenophora, Peritrichida), a ciliate with ectosymbiotic, chemoautotrophic bacteria. Eur. J. Protistol. **32**, 202–215

Berg, C. and Atalo, P. (1984) Potential of chemosynthesis in molluscan mariculture. Aquaculture **39**, 165–179

Cary, S.C. and Stein, J.L. (1998) Spanning the thermal limits: an extreme eurythermal symbiosis. In proceedings of the first international symposium on deep-sea hydrothermal vent biology. Cah. Biol. Mar. **39**, 275–278

Cavanaugh, C.M. (1983) Symbiotic chemoautotrophic bacteria in marine invertebrates from sulphide-rich habitats. Nature **302**, 58–61

Cavanaugh, C.M. (1985) Symbioses of chemoautotrophic bacteria and marine invertebrates from hydrothermal vents and reducing sediments. Biol. Soc. Wash. Bull. **6**, 373–388

Crozier, P.A. (1995) Quantitative elemental mapping of materials by energy-filtered imaging. Ultramicroscopy **58**, 157–174

Deming, J.W., Reysenbach, A.L., Macko, S.A. and Smith, C.R. (1997) Evidence for the microbial basis of a chemoautotrophic invertebrate community at a whale fall on the deep seafloor: Bone-colonizing bacteria and invertebrate endosymbionts. Microsc. Res. Tech. **37**, 162–170

Desbruyères, D., Gaill, F., Laubier, L., Prieur, D. and Rau, G.H. (1983) Unusual nutrition of the 'pompei worm' *Alvinella pompejana* (polychaetous annelid) from a hydrothermal vent environment: SEM, TEM, ^{13}C and ^{15}N evidence. Mar. Biol. **75**, 201–205

Egerton, R.F. (1986) Applications of energy-loss spectroscopy. Electron Energy-Loss Spectroscopy in the Electron Microscope (Egerton, R.F., ed.), pp.291–352, Plenum, New-York

Felbeck, H., Childress, J.J. and Somero, G.N. (1981) Calvin-benson cycle and sulphide oxidation enzymes in animals from sulphide-rich habitats. Nature **293**, 291–293

Frenkiel, L. and Mouëza, M. (1995) Gill ultrastructure and symbiotic bacteria in *Codakia orbicularis* (Bivalvia, Lucinidae). Zoomorphology **115**, 51–61

Gabe, M. (1968) Techniques Histologiques. Masson, Paris

Giere, O., Rhode, B. and Dubilier, N. (1988) Structural peculiarities of the body wall of *Tubificoides benedii* (Oligochaeta) and possible relations to its life in sulphidic sediments. Zoomorphology **108**, 29–39

Gros, O. and Maurin, L.C. (2008) Easy flat embedding of oriented samples in hydrophilic resin (LR White) under controlled atmosphere: application allowing both nucleic acid hybridizations (CARD-FISH) and ultrastructural observations. Acta Histochem. **110**, 427–431

Herzberg, G. (1945) Molecular Spectra and Molecular Structure II: Infrared and Raman spectra of polyatomic molecules. Van Nostrand, New York

Himmel, D. (2005) Application de la microspectrométrie Raman à la mesure in situ de paramètres physiques régnant dans un contact sphère/plan en régime de lubrification elastohydrodynamique. PhD Thesis, Université des Antilles et de la Guyane

Hopper, B.E. and Cefalu, R.C. (1973) Free-living nematodes from Biscayne Bay, Florida, *V. stilbonematinae*: contributions to the taxonomy and morphology of the genus *Eubostrichus greeff* and related genera. Trans. Am. Micros. Soc. **4**, 578–591

Lawry, N.H., Jani, V. and Jensen, T.E. (1981) Identification of the sulfur inclusion body in *Beggiatoa alba* B18LD by energy-dispersive X-ray microanalysis. Curr. Microbiol. **6**, 71–74

Lechaire, J.-P., Frébourg, G., Gaill, F. and Gros, O. (2006) *In situ* localization of sulfur in the thioautotrophic symbiotic model *Lucina pectinata* (Gmelin, 1791) by cryo-EFTEM microanalysis. Biol. Cell **98**, 163–170

Lechaire, J.-P., Frébourg, G., Gaill, F. and Gros, O. (2008) *In situ* characterization of sulfur in gill-endosymbionts of the shallow water lucinid *Codakia orbicularis* (Linné, 1758) by cryo-EFTEM microanalysis. Mar. Biol. **154**, 693–700

Long, D.A. (1977) Raman Spectroscopy. McGraw-Hill, U.K.

Ott, J.A. and Novak, R. (1989) Living at an interface: Meiofauna at the oxygen/sulfide boundary of marine sediments. In Reproduction, Genetics and Distributions of Marine Organisms (Ryland, J.S. and Tyler, P.A., eds), pp. 415–422, Olsen and Olsen, Fredensborg, Denmark

Ott, J.A., Novak, R., Schiemer, F., Hentschel, U., Nebelsick, M. and Polz, M. (1991) Tackling the sulfide gradient: a novel strategy involving marine nematodes and chemoautotrophic ectosymbionts. Mar. Ecol. **12**(3), 261–279

Ott, J.A., Bright, M. and Bulgheresi, S. (2004) Symbioses between marine nematodes and sulfur-oxidizing chemoautotrophic bacteria. Symbiosis **36**, 103–126

Pasteris, J.D., Freeman, J.J., Goffredi, S.K. and Buck, K.R. (2001) Raman spectroscopic and laser scanning confocal microscopic analysis of sulfur in living sulfur-precipitating marine bacteria. Chem. Geol. **180**, 3–18

Poborchii, V.V. (1996) Polarized Raman and optical absorption spectra of the mordenite single crystals containing sulfur, selenium, or tellurium in the one-dimensional nanochannels. Chem. Phys. Lett. **251**, 230–234

Polz, M.F. and Cavanaugh, C.M. (1995) Dominance of one bacterial phylotype at a mid-atlantic ridge hydrothermal vent site. Proc. Natl. Acad. Sci. U.S.A. **92**, 7232–7236

Polz, M.F., Harbison, C. and Cavanaugh, C.M. (1999) Diversity and heterogeneity of epibiotic bacterial communities on the marine nematode *Eubostrichus dianae*. Appl. Environ. Microbiol **65**, 4271–4275

Polz, M.F., Felbeck, H., Novak, R., Nebelsick, M. and Ott, J.A. (1992) Chemoautotrophic, sulfur-oxidizing symbiotic bacteria on marine nematodes: morphological and biochemical characterization. Microb. Ecol. **24**, 313–329

Polz, M.F., Distel, D.L., Zarda, B., Amann, R., Felbeck, H., Ott, J.A. and Cavanaugh, C.M. (1994) Phylogenetic analysis of a highly specific association between ectosymbiotic, sulfur-oxidizing bacteria and a marine nematode. Appl. Environ. Microbiol. **60**, 4461–4467

Reid, R.G.B. (1990) Evolutionary implications of sulphide-oxidizing symbioses in bivalves. In The Bivalvia: Proceedings of a Memorial Symposium in Honour of Sir C.M. Yonge, Edinburgh, 1986 (Morton, B., ed.), pp. 127–140, University Press, Hong-Kong

Rinke, C., Schmitz-Esser, S., Stoecker, K., Nussbaumer, A.D., Molnar, D.A., Vanura, K., Wagner, M., Horn, M., Ott, J.A. and Bright, M. (2006) '*Candidatus Thiobios zoothamnicoli*', an ectosymbiotic bacterium covering the giant marine ciliate *Zoothamnium niveum*. Appl. Environ. Microbiol. **72**, 2014–2021

Truchet, M., Ballan-Dufranc□ais, C., Jeantet, A., Lechaire, J.P. and Cosson, R. (1998) The trophosome of the vestimentifera *Riftia pachyptila* and *Tevnia jerichonana*: metal bioaccumulations and sulphur metabolism. Cah. Biol. Mar. **39**, 129–141

Vetter, R.D. (1985) Elemental sulfur in the gills of three species of clams containing chemoautotrophic symbiotic bacteria: a possible inorganic energy storage compound. Mar. Biol. **88**, 33–42

Vetter, R.D. (1991) Symbiosis and the evolution of a novel trophic strategies: thiotrophic organisms at hydrothermal vents. In Symbiosis as a Source of Evolutionary Innovation: Speciation and Morphogenesis (Margulis, L. and Fester, R., eds), pp. 219–248, MIT Press, Cambridge, MA

White, S.N., Dunk, R.M., Peltzer, E.T., Freeman, J.J. and Brewer, P.G. (2006) *In situ* Raman analyses of deep-sea hydrothermal and cold seep systems (Gorda Ridge and Hydrate Ridge). Geochem. Geophys. Geosyst. **7**, 1–12

Zbinden, M., LeBris, N., Gaill, F. and Compére, P. (2004) Distribution of bacteria and associated minerals in the gill chamber of the vent shrimp *Rimicaris exoculata* and related biogeochemical processes. Mar. Ecol. Prog. Ser. **284**, 237–251

Received 2 April 2008/26 June 2008; accepted 3 July 2008

Published as Immediate Publication 29 July 2008, doi:10.1042/BC20080051